Original Article

A Randomized, Phase 1, Placebo-Controlled Trial of APG-157 in Oral Cancer Demonstrates Systemic Absorption and an Inhibitory Effect on Cytokines and Tumor-Associated Microbes

Saroj K. Basak, PhD[1]; Alakesh Bera, PhD[2]; Alexander J. Yoon, MS[3]; Marco Morselli, PhD[4]; Chan Jeong, BS[1]; Anela Tosevska, PhD[4]; Tien S. Dong, MD[5]; Michael Eklund, BS[2]; Eric Russ, BS[2]; Hassan Nasser, MD[6]; Venu Lagishetty, PhD [5]; Rong Guo, MS[7]; Dipti Sajed, MD, PhD[8]; Sharmila Mudgal, MD, MPH[9]; Parag Mehta, PhD[9]; Luis Avila, PhD[9]; Meera Srivastava, PhD[2]; Kym Faull, PhD[3]; Jonathan Jacobs, MD, PhD[5]; Matteo Pellegrini, PhD[4,10,11]; Daniel Sanghoon Shin, MD, PhD[10,12]; Eri S. Srivatsan, PhD[1,10,11]; and Marilene B. Wang, MD [1,6,10]

BACKGROUND: Although curcumin's effect on head and neck cancer has been studied in vitro and in vivo, to the authors' knowledge its efficacy is limited by poor systemic absorption from oral administration. APG-157 is a botanical drug containing multiple polyphenols, including curcumin, developed under the US Food and Drug Administration's Botanical Drug Development, that delivers the active components to oromucosal tissues near the tumor target. **METHODS:** A double-blind, randomized, placebo-controlled, phase 1 clinical trial was conducted with APG-157 in 13 normal subjects and 12 patients with oral cancer. Two doses, 100 mg or 200 mg, were delivered transorally every hour for 3 hours. Blood and saliva were collected before and 1 hour, 2 hours, 3 hours, and 24 hours after treatment. Electrocardiograms and blood tests did not demonstrate any toxicity. **RESULTS:** Treatment with APG-157 resulted in circulating concentrations of curcumin and analogs peaking at 3 hours with reduced IL-1β, IL-6, and IL-8 concentrations in the salivary supernatant fluid of patients with cancer. Salivary microbial flora analysis showed a reduction in *Bacteroidetes* species in cancer subjects. RNA and immunofluorescence analyses of tumor tissues of a subject demonstrated increased expression of genes associated with differentiation and T-cell recruitment to the tumor microenvironment. **CONCLUSIONS:** The results of the current study suggested that APG-157 could serve as a therapeutic drug in combination with immunotherapy. ***Cancer* 2020;0:1-15**. © *2020 American Cancer Society*.

LAY SUMMARY:

- Curcumin has been shown to suppress tumor cells because of its antioxidant and anti-inflammatory properties. However, its effectiveness has been limited by poor absorption when delivered orally.
- Subjects with oral cancer were given oral APG-157, a botanical drug containing multiple polyphenols, including curcumin. Curcumin was found in the blood and in tumor tissues. Inflammatory markers and *Bacteroides* species were found to be decreased in the saliva, and immune T cells were increased in the tumor tissue.
- APG-157 is absorbed well, reduces inflammation, and attracts T cells to the tumor, suggesting its potential use in combination with immunotherapy drugs.

KEYWORDS: APG-157, curcumin, gene expression, head and neck cancer, salivary microbiome, systemic absorption, T-cell recruitment.

INTRODUCTION

Head and neck (H&N) cancer includes the oral cavity, pharynx, larynx, paranasal sinus, nasal cavity, and salivary glands, with squamous cell carcinoma being the major disease phenotype.[1] Worldwide, the disease accounts for approximately 650,000 cases and 330,000 deaths annually,[2] and statistics provided by the American Society of Clinical Oncology indicate that 53,000 to 65,410 individuals in the United States will develop H&N cancer, and 10,800 to 14,620 will

Corresponding Author: Marilene B. Wang, MD, Department of Surgery, Veterans Administration Greater Los Angeles Healthcare System, David Geffen School of Medicine, University of California at Los Angeles, Los Angeles, CA 90073 (mbwang@g.ucla.edu).

[1]Department of Surgery, Veterans Administration Greater Los Angeles Healthcare System, David Geffen School of Medicine, University of California at Los Angeles, Los Angeles, California; [2]Department of Anatomy, Physiology and Genetics, Uniformed Services University of Health Sciences, Bethesda, Maryland; [3]Pasarow Mass Spectrometry Laboratory, Jane and Terry Semel Institute for Neuroscience and Human Behavior, Department of Psychiatry and Biobehavioral Sciences, David Geffen School of Medicine, University of California at Los Angeles, Los Angeles, California; [4]Department of Molecular, Cell and Developmental Biology, University of California at Los Angeles, Los Angeles, California; [5]Division of Gastroenterology, Hepatology and Parenteral Nutrition, Department of Medicine, Veterans Administration Greater Los Angeles Healthcare System, David Geffen School of Medicine, University of California at Los Angeles, Los Angeles, California; [6]Department of Head and Neck Surgery, David Geffen School of Medicine, University of California at Los Angeles, Los Angeles, California; [7]Department of Medicine Statistics Core, David Geffen School of Medicine, University of California at Los Angeles, Los Angeles, California; [8]Department of Pathology, David Geffen School of Medicine, University of California at Los Angeles, Los Angeles, California; [9]Aveta Biomics Inc, Bedford, Massachusetts; [10]Jonsson Comprehensive Cancer Center, University of California at Los Angeles, Los Angeles, California; [11]Molecular Biology Institute, University of California at Los Angeles, Los Angeles, California; [12]Division of Hematology-Oncology, Department of Medicine, VA Greater Los Angeles Healthcare System, David Geffen School of Medicine, University of California at Los Angeles, Los Angeles, California

Additional supporting information may be found in the online version of this article.

DOI: 10.1002/cncr.32644, **Received:** September 9, 2019; **Revised:** October 16, 2019; **Accepted:** October 20, 2019, **Published online** Month 00, 2019 in Wiley Online Library (wileyonlinelibrary.com)

die of the disease each year.[3,4] In the United States, H&N cancer accounts for approximately 4% of all cancers.[5] The main risk factors associated with H&N cancer are smoking, alcohol consumption, and infections with the human papillomavirus and Epstein-Barr virus. The choice of treatment (surgery, chemotherapy, radiotherapy, targeted therapy, or their combinations) depends on the disease phenotype and stage and patient comorbidities. The most widely used chemotherapeutic agents include platinum-based compounds (cisplatin, carboplatin),[6] taxanes (docetaxel, paclitaxel),[7] methotrexate,[8] 5-fluorouracil,[9] and cetuximab.[10] Recently, patients with advanced H&N cancer were treated successfully with immune checkpoint blockade antibodies (pembrolizumab or nivolumab) as a subsequent therapeutic option.[11,12] However, the rate of recurrence of localized squamous cell carcinoma of the H&N (SCCHN) is approximately 10% to 20%,[13] and the incidence of locally advanced SCCHN is approximately 50%.[14] Patients with recurrent or metastatic SCCHN have a poor prognosis, and the median overall survival is <1 year.[15] Thus, there is a need for new therapies to effectively treat this devastating disease.

The majority of current drug development efforts separately and independently have focused on agents that target a single or a few biological pathways. Eventually, the activity of a therapeutic agent against one target or pathway often fails to provide a durable clinical response because the biological systems often compensate by establishing secondary pathways. However, although the current clinical practice of drug combinations is common, the pharmaceutically compounded active molecules, when combined, often lack synergy and may increase the incidence of adverse events.

Plants evolved to produce secondary metabolites while adapting to countless abiotic and biotic stresses, including those from mammals. The co-evolved molecules, often produced from common biosynthetic pathways, have a great deal of structural similarity and demonstrate biological synergy. Unlike the majority of synthetic drugs, minor but meaningful differences in the functional groups on the co-evolved molecules contribute to an unprecedented ligand binding versatility. In this regard, plant secondary metabolites represent field-tested combination therapeutics consisting of naturally synergistic molecules capable of effecting multiple biological targets and pathways.

One medicinally important plant is *Curcuma longa*. Turmeric, from the rhizome of this plant, contains by dry weight approximately 60% to 70% carbohydrate, 6% to 13% water, 6% to 8% protein, 5% to 10% fat, 3% to 7% dietary minerals, 3% to 7% essential oils, 2% to 7% dietary fiber, and 1% to 6% flavonoids, primarily consisting of polyphenols (curcuminoids).[16] Over the past 20 years, curcumin and its derivatives have been studied as an alternative supplemental therapy for human cancers, including those of the breast, cervix, pancreas, and colorectum.[17,18] The predominant curcuminoid in turmeric is curcumin (diferuloylmethane, up to 3% of the dry weight of turmeric), with smaller amounts of bis-demethoxycurcumin (BDC) and dimethoxycurcumin (DMC).[19] Several structurally related compounds, such as difluorinated curcumin (CDF) and cinnamic, p-coumaric, syringic, ferulic, and caffeic acids, also have anti-inflammatory, antioxidative, and anticancer properties.[20] Our in vitro and in vivo studies with nude mice xenografts demonstrated that liposome-encapsulated curcumin and CDF had anticancer effects associated with a reduction in the concentrations of cytokines and cancer stem cell markers.[21-23]

A search of the ClinicalTrials.gov website (https://clinicaltrials.gov/), a database of privately and publicly funded clinical studies conducted or recently completed around the world, conducted in April 2019 using the word "curcumin" generated 195 hits, 64 of which were cancer-related trials. However, in the United States, only 32 curcumin-related and cancer-related trials were listed, with only 1 trial listed as completed for patients with H&N cancer (curcumin biomarker, 2010-2016).

Although the effect of curcumin on diseases is known through in vitro and preclinical studies, clinical studies are hampered due to poor systemic absorption after oral administration. This could be attributed to the first (intestine) and second (liver) pass effects that may result in degradation or rapid clearance of curcumin, its derivatives, and their metabolites.[24] To the best of our knowledge, the precise mechanism of curcumin action is not clearly understood, although inhibition of growth factor–induced proliferation, suppression of cell cycle processes, and induction of apoptosis through mitochondrial-dependent[25] and mitochondrial-independent pathways[26] have been proposed.

The oral microbiome may play a role in cancer development, and it has been implicated in cancer progression.[27] Indeed, inflammation is considered a key feature of chronic diseases including cancer, and it has been proposed that bacterial infection influences inflammation and promotes cancer development.[28] Several studies have indicated that changes in the oral microbiota are associated with oral squamous cell carcinoma (OSCC), and this also has been used for diagnosis.[29] It also has been shown that there may be potential associations between the oral

microbiome and mutational changes in OSCC linked to variations in the relative abundance of *Firmicutes* and *Bacteroidetes* species.[30] Recently, small subunit ribosomal RNA (16S rRNA) studies have been used to identify oral bacterial taxonomic lineages and microbial differences between patients with cancer and normal subjects.[31] Changes in the oral microbiome and their association with surgical resection also have been reported in oral cancer progression.[32]

To the best of our knowledge, the majority of the studies focused on curcumin and cancer were in keeping with the conventional reductionist paradigm of using a single drug designed to modulate a single or a few targets. However, in traditional botanical medicine, it is the combination of multiple molecules working synergistically that is responsible for the pharmacological effect and likely to provide a durable clinical response. Therefore, APG-157 was designed on the principles of systems biology and polypharmacology. It contains all the major polyphenols occurring naturally in *Curcuma longa* and is encased in a pastille, an oromucosally deliverable hydrogel. Although the importance of the local effect of the drug on the tumor always has been appreciated, to our knowledge currently all drugs approved for H&N cancer are administered intravenously. APG-157 is a first-in-class botanical drug developed under the US Food and Drug Administration's Botanical Drug Development that delivers the active components to oromucosal tissues near the H&N tumor target.

The study laboratory has explored the possibility of using curcumin as an alternative adjunct therapy for patients with H&N cancer. These studies have demonstrated the antitumor effects of curcumin, both in vitro and in a preclinical mouse model of xenograft tumors, and anti-inflammatory effects as measured after short-term oral treatment of normal subjects and patients with H&N cancer.[21-23,33] The primary objectives of the current randomized, double-blind, placebo-controlled trial of APG-157 were to determine the pharmacokinetics and safety of the orally delivered pastille when used by normal subjects and patients with cancer. The study was designed to determine the effects on cytokine concentrations and on the microbial community of the oral mucosa. Furthermore, tumor tissues from before and after APG-157 treatment of a patient with cancer were studied to determine the effect of the drug on the tumor cell molecular phenotype. In the current study, we have presented evidence that APG-157 is well tolerated and warrants an extended clinical trial to assess its usefulness as an adjuvant therapeutic drug.

MATERIALS AND METHODS

Details of the procedures and the methods are presented in the Supporting Materials and are described briefly below.

Study Population

The investigation was performed after approval from the institutional review board (IRB) of the Veterans Administration Greater Los Angeles Healthcare System (VAGLAHS) in Los Angeles, California. Subject recruitment and drug treatments followed the protocols approved by the VAGLAHS IRB. The normal and cancer cohorts were recruited from the ear, nose, and throat clinics at VAGLAHS. Inclusion criteria were age >18 years, English fluency, and no history of prior chemotherapy or radiotherapy, or inflammatory conditions of the oral cavity or oropharynx. Patients with cancer had biopsy proven OSCC. One of the patients with cancer (patient 1*) was included in the study with advanced cancer of the floor of the mouth and underwent surgery for tumor removal 24 hours after the completion of the study. His prestudy biopsy and poststudy surgically removed normal and tumor tissues were available to determine the effect of treatment on tumor cells.

Cancer staging and exclusion criteria of the study are included in detail in the Supporting Materials.

Study Product

APG-157, which contains turmeric extract, is a proprietary, patent-pending, drug product developed by Aveta Biomics Inc. The drug substance, derived from the plant *Curcuma longa*, differs from other turmeric products in its use of a complete unfractionated herb extract, and is encapsulated in a soft lozenge, a hydrogel-based drug delivery system. APG-157 slowly disintegrates in the oral cavity over 15 to 20 minutes to release the drug substance. The drug substance is a precise, rational combination of multiple molecules derived from *Curcuma longa* wherein curcumin is the principal component. It is produced by the biofractionation of the rhizome of *Curcuma longa* under current good manufacturing practice (cGMP) conditions to meet US Food and Drug Administration Chemistry, Manufacturing, and Controls guidance ensuring the consistency and quality of the pharmaceutical grade product. Each APG-157 lozenge contains 100 mg of the drug substance.

Study Design and Procedure

Two different dosages of the drug (APG-157) or placebo control gelatin pastilles, 3 × 100 mg and 3 × 200 mg, were tested (Fig. 1). A total of 32 subjects were enrolled,

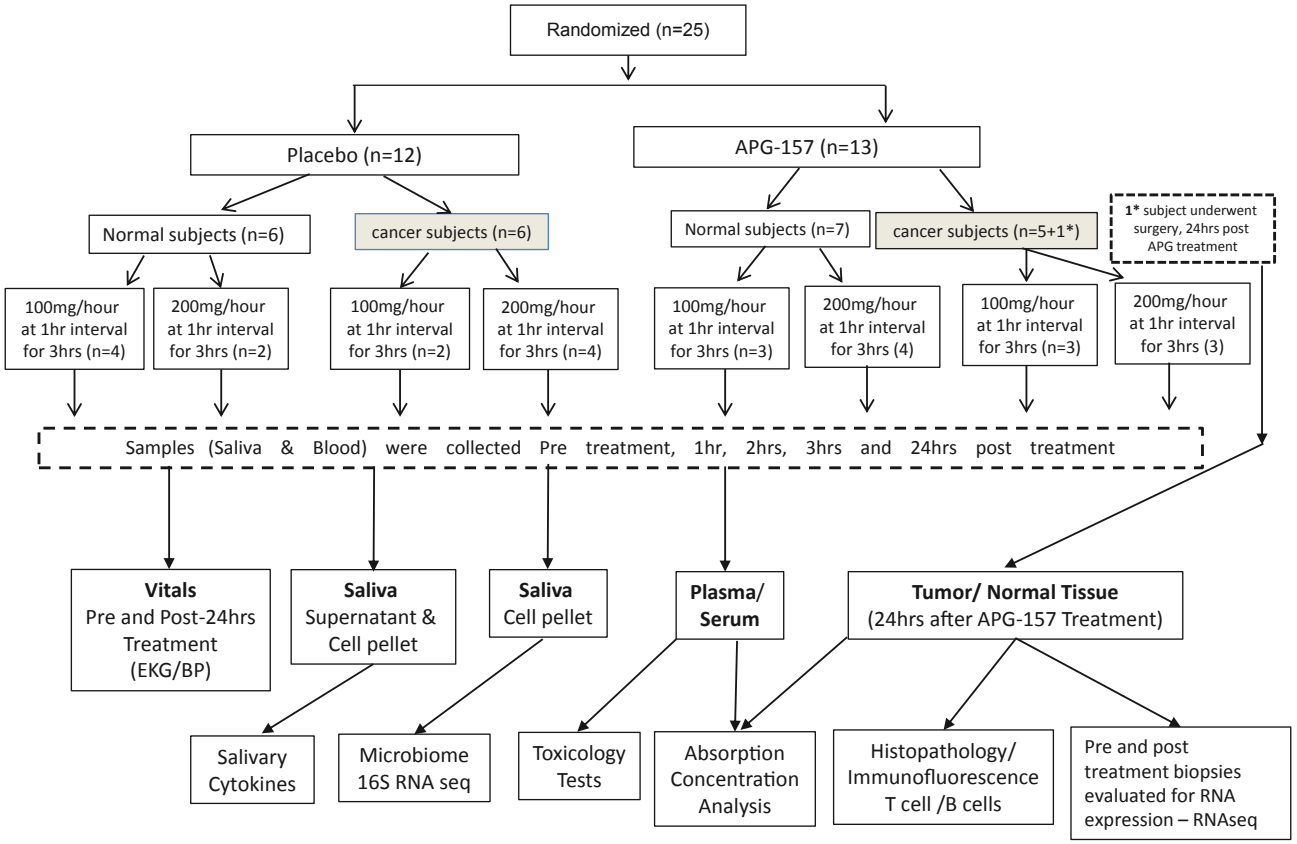

Figure 1. A Randomized Double-Blind, Placebo-Controlled Trial of APG-157 in healthy adult and oral squamous cell carcinoma subjects.

and 25 completed the study (see Supporting Fig. 1A): 13 normal individuals (4 in the 100-mg placebo control group and 3 in the 100-mg APG-157 treatment group and 2 in the 200-mg placebo group and 4 in the 200-mg APG-157 treatment group) and 12 patients with oral cancer (2 in the 100-mg placebo control group and 3 in the 100-mg APG-157 treatment group and 4 in the 200-mg placebo control group and 3 in the 200-mg APG-157 treatment group). The drug was delivered transorally each hour for 3 consecutive hours for a 1-day treatment. Blood and saliva were collected before treatment and each hour after treatment (3 collections), and 1 sample was collected 24 hours after treatment (Fig. 1).

Blood collection

A nurse practitioner collected blood using an IRB-approved procedure (Fig. 1). Serum was isolated using the appropriate collection tube. At least 5 mL of blood was collected at each time point to obtain 2 mL of serum. Collections caused minimal pain and the subjects did not report any after effects.

Saliva collection

Saliva was collected before and after treatment at 1-hour intervals (3 collections) (Fig. 1). Briefly, 10 mL of saliva was collected in 50-mL tubes and kept in ice until completion of the 3-hour collection. The samples were centrifuged (500 × g for 15 minutes) and the supernatant fluid and pellets were frozen in aliquots and stored at -80 °C until analysis.

Evaluation of toxicity and/or adverse effects

Electrocardiograms were performed before treatment and 24 hours after treatment and read by a VAGLAHS cardiologist. Aliquots of serum (200 μL) were used for kidney and liver function tests at the department of pathology and laboratory medicine of the VAGLAHS.

Measurement of curcumin and analogs in blood and tissue

Serum and tissue samples were evaluated for curcumin, DMC, bisdemethoxycurcumin (BDMC), tetrahydrocurcumin (THC), glucuronidated curcumin (CG),

DMC-glucuronide (DMCG), and BDMC-glucuronide (BDMCG) concentrations with hexadeuterated curcumin as an internal standard using a highly sensitive combined liquid chromatography/mass spectrometry method as described in the Supporting Materials.

Cytokine analysis

The preparation of salivary cell and supernatant fluid samples and the measurement of cytokine concentrations were performed following an established protocol using the Meso Scale discovery platform.[33]

Microbiome profiling

To determine the oral microbial community composition, salivary cells were assayed using the 16S rRNA sequence. Extraction and sequencing of the 16S rRNA gene were performed as previously described.[34]

RNA-Seq analysis

Formalin-fixed, paraffin-embedded (FFPE) prebiopsy tissues and tissue (tumor and adjacent normal tissue) after APG-157 treatment from one of the patients with cancer was evaluated for gene expression by RNA-Seq analysis using an established protocol.

Multiplex immunofluorescence analysis

The normal, tumor, and lymph node FFPE tissues from the patient with cancer were stained for hematoxylin and eosin and were evaluated for T cells (CD4 and CD8 cells), PD-L1, and PD-1 expression by established histology and immunostaining methods.

Statistical Analysis

Salivary cytokine data (IL-6, IL-8, TNF-α, and other cytokine levels) were analyzed using a Fisher exact test. Chi-square and Student *t* tests were performed for the RNA-Seq data. For the microbiome, alpha diversity metrics included the Faith phylogenetic diversity metric, Chao1 function, and Shannon index. The significance of differences in alpha diversity was calculated using a 2-tailed Student *t* test. Beta diversity was calculated using square root Jensen-Shannon divergence and visualized using principal coordinates analysis. Adonis, a permutational analysis of variance, was performed using 10,000 permutations to test for differences in square root Jensen-Shannon divergence distances between drug and placebo controlling for cancer, subject, and timing of the sample collection. Associations between microbial genera with cancer, treatment, time, and dose were evaluated using DESeq2 in R statistical software, which uses an empirical Bayesian approach to shrink dispersion and fit nonrarified count data to a negative binomial model.[35] *P* values for differential abundance were converted to q values to correct for multiple hypothesis testing (<.05 for statistical significance).[36]

RESULTS

APG-157 Treatment Did Not Result in Local or Systemic Toxicity

A total of 13 normal subjects and 12 subjects with oral cancer participated in the study (age range, 33-75 years) (Fig. 1) (see Supporting Fig. 1). Four subjects in the placebo group and 3 subjects in the APG-157 group withdrew from the study. Of the 25 subjects, 12 received placebo control and 13 received active drug APG-157 (Fig. 1). None of the subjects reported adverse effects from any of the procedures used in the current study.

Electrocardiogram results evaluated for PR wave delay did not demonstrate a significant delay in any of the subjects, except in 1 normal subject who received 100 mg of APG-157, in whom a PR delay of 24 milliseconds at 24 hours after treatment was observed. This was deemed to be within the normal range of variation. The serum samples from the 25 subjects did not demonstrate any abnormalities with regard to blood counts, electrolytes, or liver or kidney functions except for a preexisting condition or some minor variations.

Transoral APG-157 Treatment Results in Systemic Curcumin Absorption

Despite considerable variation between subjects with regard to measured concentrations, curcumin, DMC, BDMC, THC, and CG were detected in the sera of all subjects after treatment with APG-157 at the 2-hour, 3-hour, and 24-hour time points. As expected, there generally were higher serum concentrations in the group treated with 200 mg of APG-157 compared with those receiving the 100-mg dose, indicating a dose-dependent effect. Curcuminoids were not detected in the sera from individuals receiving placebo. Curcumin concentrations were between 0.5 and 2 nM at the 1-hour time point, rose to a maximum of 1.5 to 13 nM at 3 hours, and declined at the 24-hour time point (Fig. 2A). The temporal display of the summed concentrations of all 5 compounds overcame to a large extent the between-subject variability and more clearly demonstrated that peak curcuminoid concentrations were reached at the 3-hour time point (Fig. 2B). This result also suggests higher concentrations of the compounds in sera from patients with cancer compared with healthy controls, although caution should be exercised herein because of the relatively small sample size.

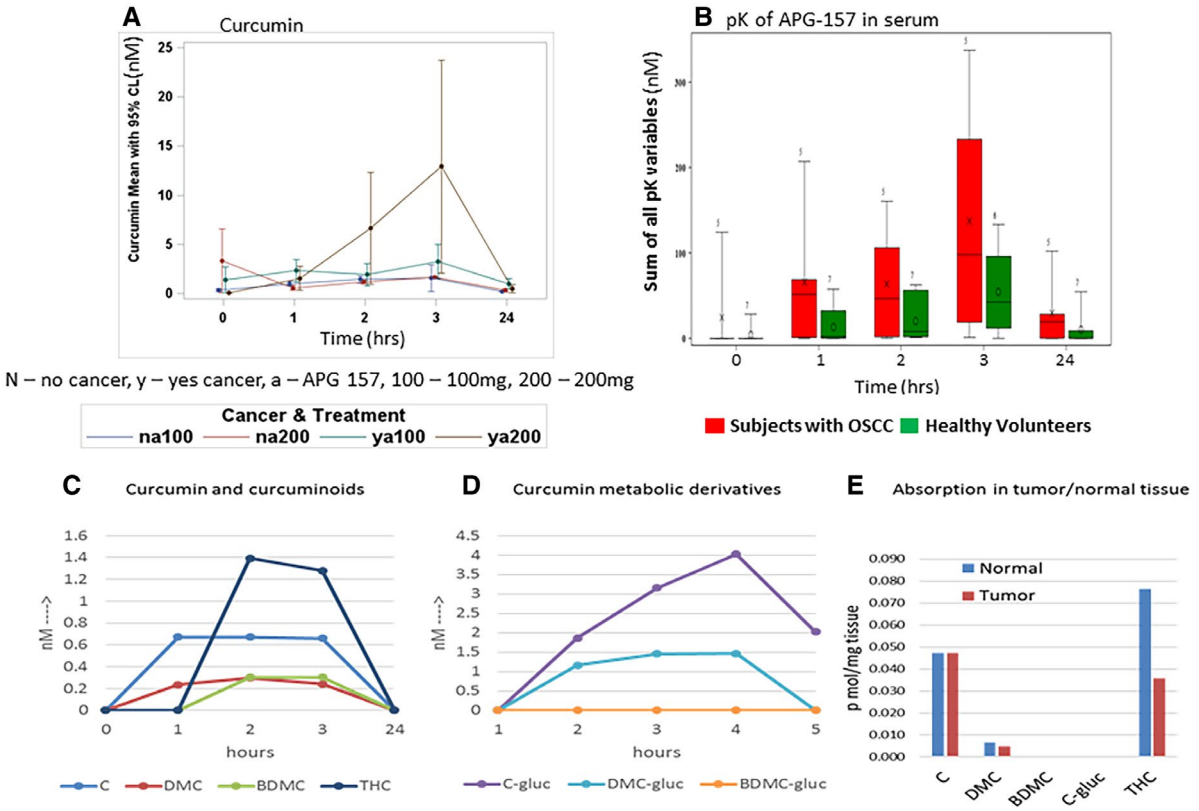

Figure 2. Systemic absorption of curcumin and its analogs in the serum of APG-157 treated subjects. Mixed model with cancer, treatment and time were used as main effects and random batch and subject effects were then fitted in. Time (hours) is included as a class variable in the model. (A) Curcumin (B) didemethoxycurcumin (DD curcumin) (C) demethoxycurcumin (DM curcumin) and (D) metabolic derivative G curcumin. (E) Combined value pK data of curcumin and analogs demonstrates systemic absorption.

One of the cancer subjects (patient 1*) who was treated with APG-157 underwent surgery for tumor removal 24 hours after treatment, and his blood and normal and tumor tissues were evaluated. The results demonstrated that the temporal serum profiles of curcumin, DMC, BDMC, and THC concentrations in this patient reached a maximum of up to 1.4 nM between 1 to 3 hours after treatment (Fig. 2C), whereas the temporal profiles of CG and DMCG in the sera reached a maximum of up to 4 nM and were slightly delayed, peaking between 3 to 24 hours after treatment (Fig. 2D). Curcumin and THC were the major curcuminoids detected in the tumor and adjacent normal tissues from this individual, with smaller amounts of DMC and undetectable amounts of BDMC and the glucuronide derivatives (Fig. 2E). These results demonstrated that transoral delivery of APG-157 results in the absorption of curcumin and its analogs in both the blood and oral tissues.

APG-157 Treatment Leads to a Reduction in Salivary Pro-Inflammatory Cytokine Concentrations

Figure 3 shows decreased cytokine concentrations of IL-8, IL-1β, and TNF-α among patients with cancer treated in the placebo versus APG-157 groups. We did not observe statistically significant differences between normal subjects, who expressed low levels of cytokines, and patients with cancer. The results for all the cytokines for both the normal subjects and patients with cancer treated with placebo or APG-157 are included in Supporting Figure 2.

Evaluation of salivary samples from cancer subject 1*, who underwent surgery after treatment, demonstrated reductions in inflammatory cytokine levels of L-12p70, IL-6, and TNF-α and an increase in the levels of IFN-γ, IL-10, IL-2, and IL-1β at 3 hours in the salivary supernatant fluid samples treated with APG-157 (see Supporting Fig. 3). The reduction in cytokine concentrations

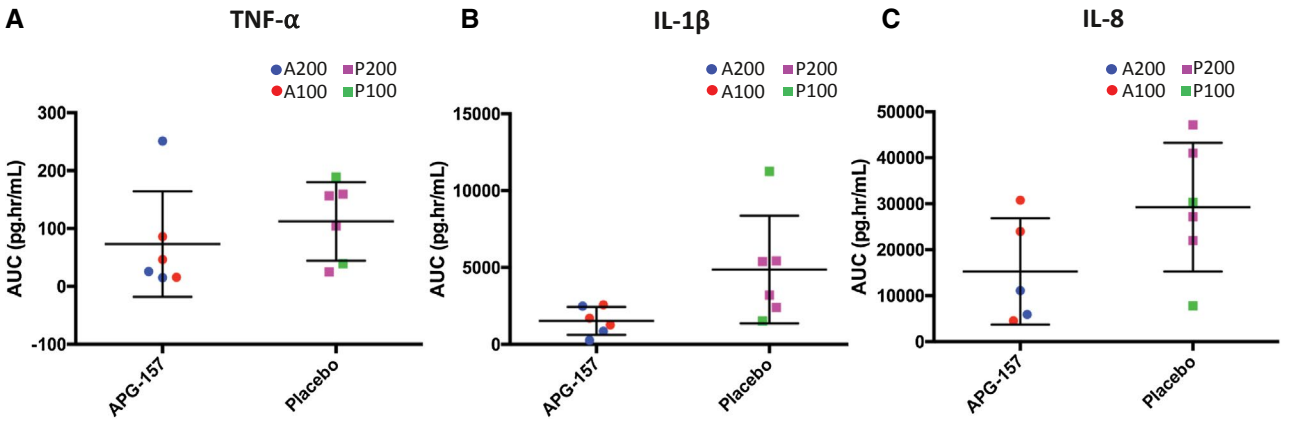

Figure 3. Reduced cytokine levels detected 24 hours post APG-157 treatment in cancer subjects. The area under the curve (AUC) of cytokines (A) TNF-α, (B) IL-1β and (C) IL-8 between 0 and 24 hours points to reduced expression of cytokines in both the 100 (A100) and 200mg (A200) treated salivary supernatant samples.

(IL-6, IL-8, IFN-γ, IL-10, granulocyte-macrophage colony-stimulating factor, IL-12p70, and TNF-α) in the cells and supernatant fluid samples 24 hours after treatment might be due to continued drug treatment after 3 hours by this subject, attributed to delayed absorption secondary to the large tumor and dry mouth conditions.

Reduction in Bacteroides in Salivary Cells Treated With APG-157

There was a statistically significant difference noted with regard to microbial composition as measured by beta diversity between patients with cancer and control subjects (Fig. 4A). There was no statistical difference noted with regard to any alpha diversity metric. However, there were many differences noted when comparing the relative abundances of patients with cancer versus control subjects at both the phyla and genus levels (Fig. 4B). Differential abundance testing was performed at the genus level to compare patients with cancer with control subjects. Figure 4C shows all the genera that were found to be statistically different (q value <.05) between patients with cancer and control subjects. Overall, there were 33 genera that were found to be different between the 2 groups, with *Fusicatenibacter*, *Dorea*, *Dialister*, *Ruminococcus*, and an unknown genus belonging to the Ruminococcaceae family comprising the genera with the highest relative abundance in patients with cancer compared with control subjects.

Similar to the differences observed between patients with cancer and controls, there also was a significant difference in the microbial composition noted between subjects who received APG-157 compared with placebo when controlling for covariates including cancer and timing of sample collection (Fig. 5A). There was no statistical difference noted with regard to any alpha diversity metric between patients treated with placebo versus APG-157, and the compositional makeup 24 hours after treatment is summarized in Figure 5B. Differential abundance testing demonstrated that 5 genera were statistically different between subjects treated with placebo versus APG-157 when controlling for the presence of cancer and the timing of sample collection (Fig. 5C). *Bacteroides* was the genus found to have the greatest relative abundance and demonstrated a clear decrease after treatment with APG-157 across time (Figure 5D). Compared with baseline values before treatment, APG-157 treatment resulted in a 56% decrease in *Bacteroides* species 24 hours after treatment with APG-157.

Analysis of the pooled data regarding the microbial population in patients with cancer who were treated with APG-157 and placebo demonstrated that there was a dose-dependent reduction in the ratio of *Firmicutes* to Bacteroidetes in subjects treated with APG-157 compared with those receiving placebo (data not shown). The ratio of *Firmicutes* to Bacteroidetes for subjects receiving 100 mg of placebo and 100 mg of APG-157 was 22% versus 82%, respectively, and was 2.3% versus 129%, respectively, for subjects receiving 200 mg of placebo and 200 mg of APG-157, indicating a concentration-dependent reduction in the *Bacteroides* population after treatment with APG-157.

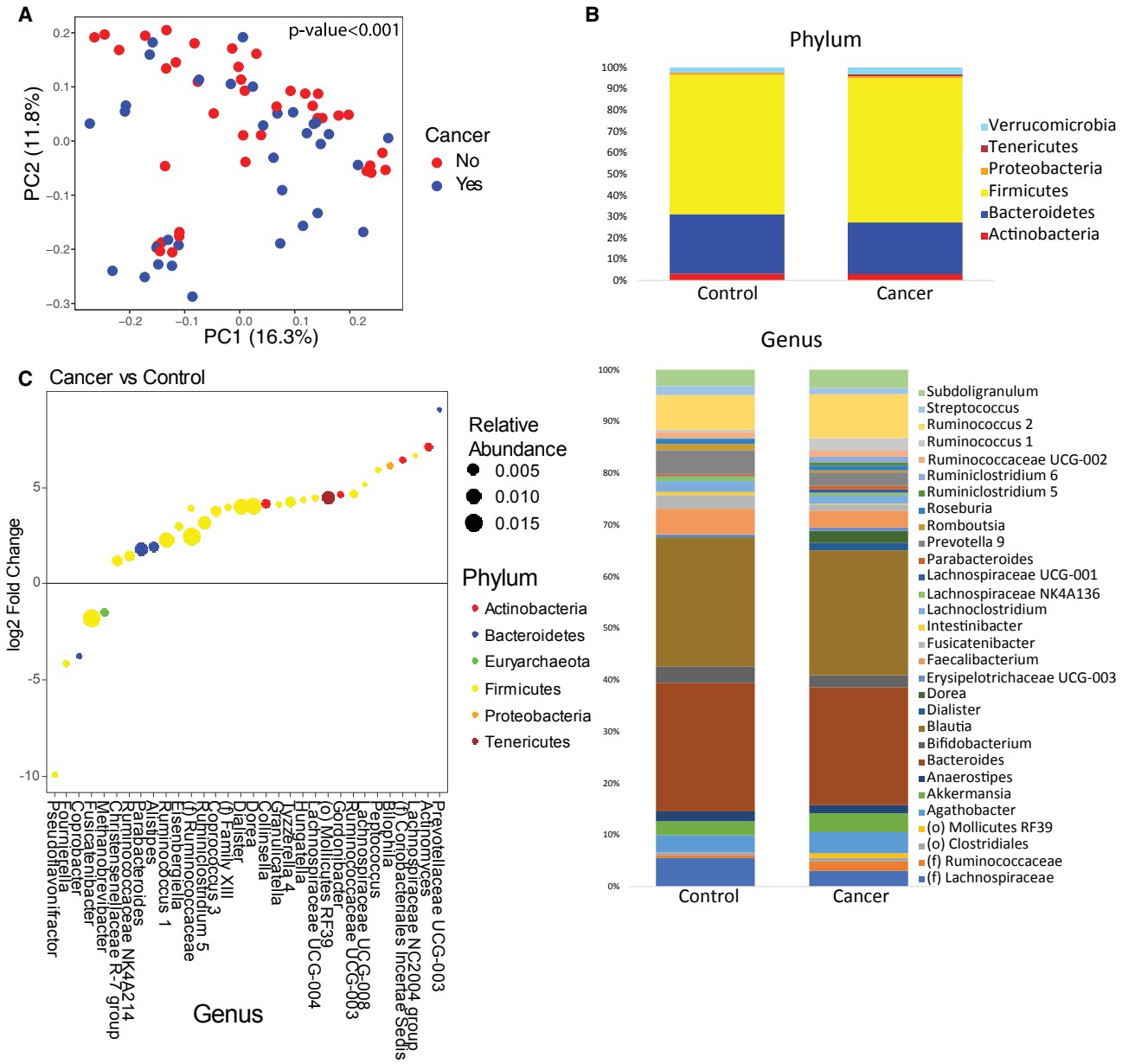

Figure 4. Microbial composition differs in cancer and normal subjects. (A) Principal coordinate analysis plot of the cancer versus control subjects with subsequent multivariate *P* values. (B) Taxonomic profiles of control and cancer subjects organized by phylum and genus. (C) Differential abundance testing of genera that are statistically different (q value <0.05) between cancer and control subjects. A positive log 2-fold change represents genera that are higher in cancer subjects as compared to control subjects.

APG-157 Treatment Results in an Alteration in the Gene Expression Pattern in Tumor Tissue

RNA-Seq analysis was performed in duplicates from FFPE normal and tumor tissues collected 2 months prior to treatment and after treatment. Due to the heterogeneous cell composition of the biopsies, gene expression–based deconvolution was performed using 2 distinct algorithms. Transcriptionally significant differences in cell and tissue composition between the adjacent normal tissue and the tumor tissue, as well as between the pretreatment biopsy and posttreatment tumor samples, were determined (Fig. 6A). Gene expression–based tissue deconvolution principal component analysis demonstrated that a large percentage of variability could be explained by principal component 1 and is due to the difference between normal tissue and pretreatment and posttreatment tumor

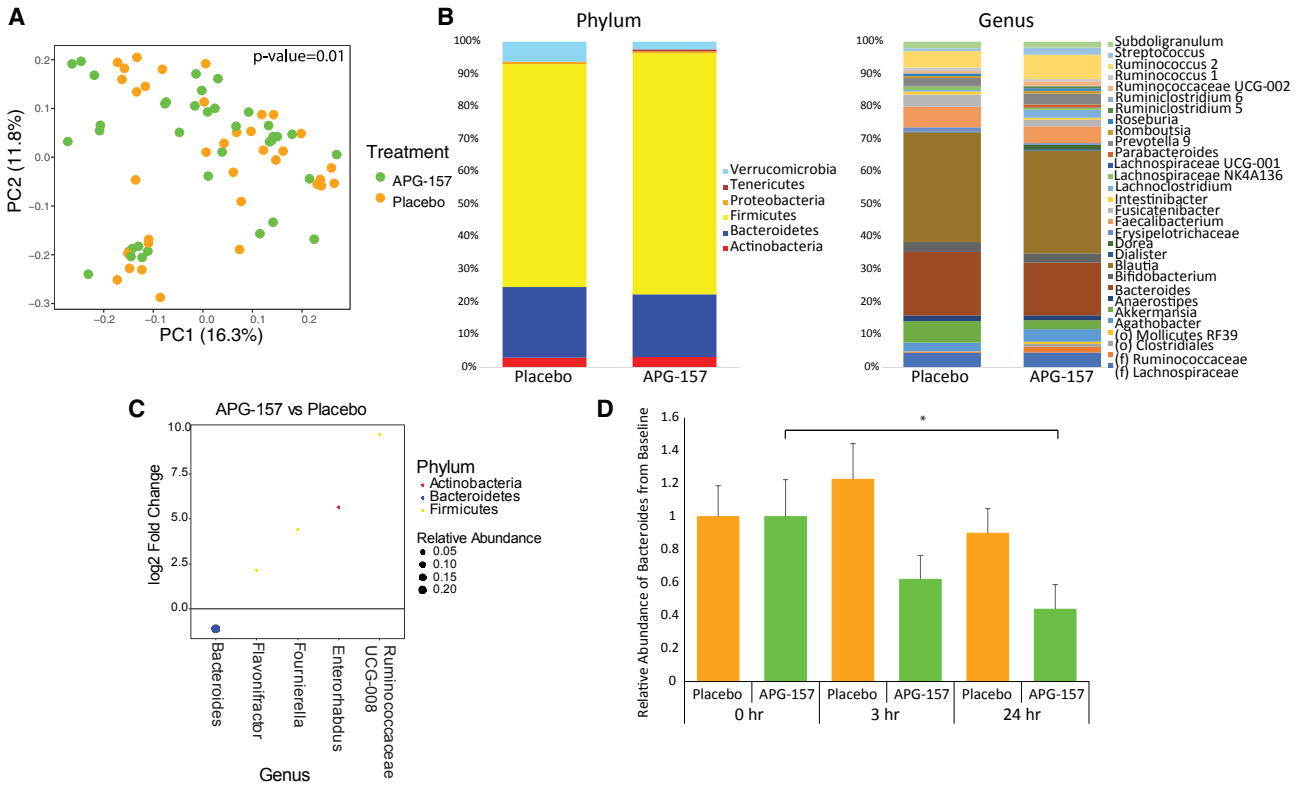

Figure 5. Decrease in *Bacteroid*es species in APG-157 treated salivary cells of cancer subjects. (A) Principal coordinate analysis plot by treatment with subsequent multivariate *P* values. (B) Taxonomic profiles of placebo versus APG-157 treated cancer subjects organized by phylum and genus. (C) Differential abundance testing of genera that are statistically different (q value <0.05) between treatment groups. A positive log 2-fold change represents genera that are higher in APG-157 treated cancer subjects as compared to placebo. (D) Representation of relative abundance of *Bacteroides* from baseline of cancer subjects treated with placebo versus APG-157 shows decrease in *Bacteroides* species in APG-157 treated salivary cells of cancer subjects.

samples (Fig. 6B.). Both Gene Expression Deconvolution Interactive Tool (GEDIT) and Signature Visualization Tool (SaVanT) perform a supervised deconvolution against a reference matrix of choice, and SaVanT in addition performs an analysis of variance test for differences in tissue type abundance between samples. Figure 6B shows the differences in tissue type composition estimated by GEDIT, which sums the estimates to 1 and therefore the results strongly depend on the number of tissues provided in the reference set. The highest percentage of signature genes detected in the normal tissue was characteristic of skeletal muscle (Fig. 6C). However, the pretreated tumor biopsy cells were enriched for bronchial epithelial and adenocarcinoma cells, and the posttreatment tumor samples demonstrated upregulation of adipocyte-specific and cardiac myocyte–specific genes.

The same analysis was performed using only the immune cell types to estimate potential immune cell infiltration in tumor or healthy tissue. Gene deconvolution for immune cell subtypes demonstrated differences in B-cell and T-cell subpopulations in the normal versus tumor tissues (see Supporting Fig. 4A). A similar analysis using SaVanT and selected tissues from the GTEx database also was performed.[37] Unlike GEDIT, SaVanT outputs scores rather than the percentages of cell populations, and the scores do not usually add up to 1. Using a built-in functionality, analysis of variance for significant differences between tissue abundances, demonstrated a significantly higher abundance of skeletal and esophageal muscle signature in the normal tissue compared with both tumor biopsies (see Supporting Fig. 4B). Conversely, the prebiopsy sample was enriched in the esophageal mucosa signature, whereas the posttreatment tumor biopsy was enriched in a transformed fibroblast tissue signature. Thus, a differential effect on gene expression was observed in posttreatment tumor cells compared with the prebiopsy tumor cells.

A

Tissue	Total Reads	DeDuplicated Reads	% Retained	Uniquely Mapped	%Mappability	Mapped To Feature	% Feature Mappability	rRNA	MT-rRNA	%rRNA
Post-normal_1	1.17E+08	6.35E+07	54.145	5.14E+07	80.969	3.25E+07	63.214	1.05E+06	1.05E+06	0.002
Post-normal_2	3.24E+07	1.16E+07	35.753	8.98E+06	77.488	5.75E+06	63.976	1.61E+05	1.61E+05	0.003
Post-tumor_1	2.51E+07	1.13E+07	45.051	8.12E+06	71.693	6.65E+06	81.918	6.39E+04	6.37E+04	0.003
Post-tumor_2	7.21E+07	3.95E+07	54.808	2.90E+07	73.461	2.39E+07	82.352	4.25E+05	4.24E+05	0.002
Prebiopsy_1	2.30E+07	7.80E+06	33.921	5.44E+06	69.686	4.56E+06	83.868	2.59E+04	2.57E+04	0.003
Prebiopsy_2	1.75E+07	5.42E+06	30.902	3.72E+06	68.561	3.11E+06	83.754	1.73E+04	1.71E+04	0.008

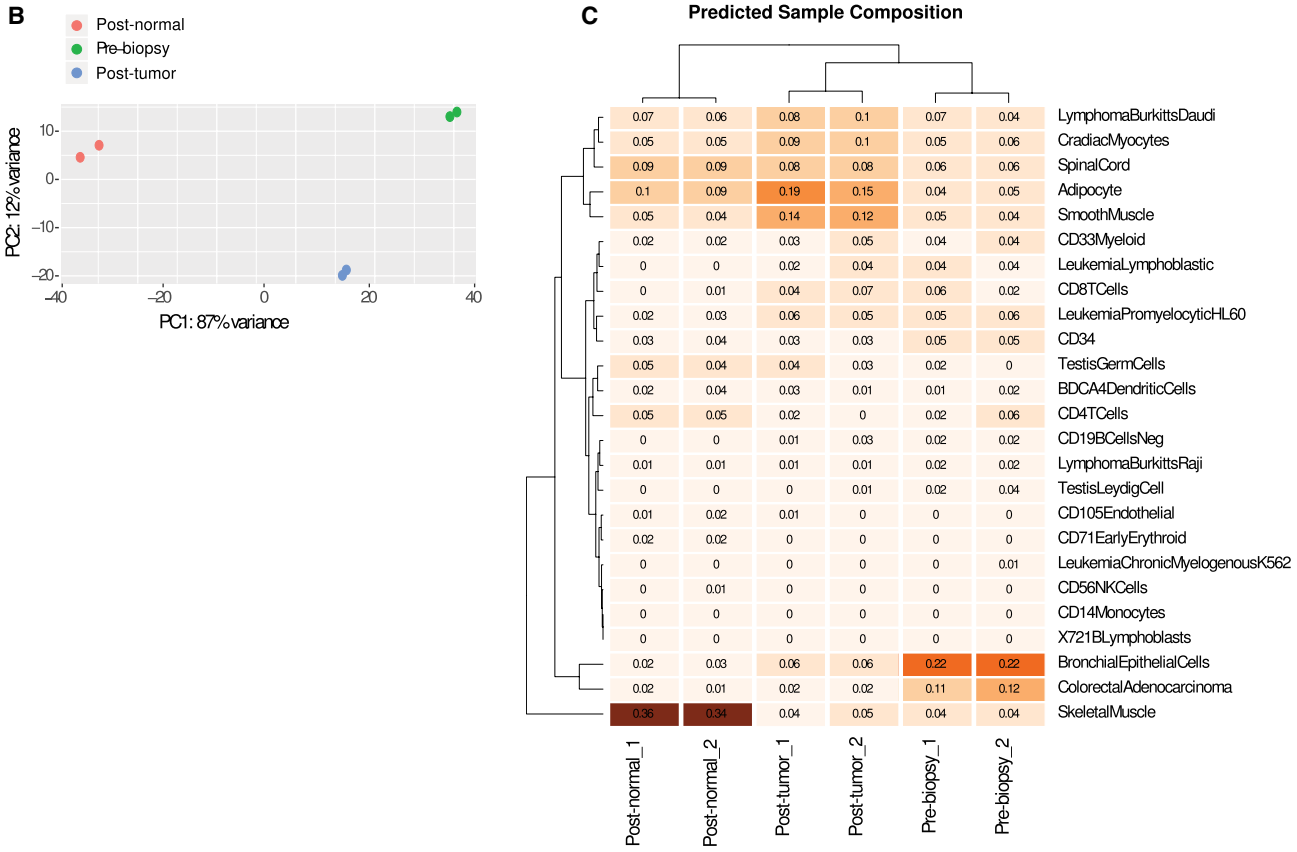

Figure 6. Differential tissue specific expression in pre and post treatment tissue samples. (A) Table with RNAseq statistics of FFPE samples points to the number of reads in each sample. (B) Unsupervised clustering of FFPE RNAseq samples and PCA plot showing the percentage of variance explained by the first two principal components. All genes with normalized counts higher than 1 for all samples were used in this analysis. Gene counts were transformed using variance-stabilization. (C) GEDIT tissue deconvolution output, using all tissues as reference.

Differential Gene Expression

Using DESeq2 genes with a Benjamini-Hochberg adjusted *P* value of <.01, an absolute fold change ≥2 was selected. In prebiopsy tumor tissue, gene ontology enrichment analysis demonstrated a significant upregulation of genes associated with cell adhesion, cell division, and the cell cycle (see Supporting Fig. 5A), and downregulation of genes related to metabolism, energy, and muscle development in prebiopsy tumor cells (see Supporting Fig. 5B). This result confirmed an increased muscle tissue signature in the normal tissue sample compared with the prebiopsy sample. Similarly, these genes and their pathways were upregulated or downregulated in posttreatment tumor tissue compared with adjacent normal tissue (see Supporting Figs. 5C and D). Although the number of significantly different genes between the pretreatment and posttreatment biopsies was lower (data not shown), some of the upregulated genes in the posttreatment tumors were involved in muscle system or vascular development, similar to the genes upregulated in normal tissues (see Supporting Figs. 5E and F). Thus, the results demonstrated a differential expression of genes after treatment with APG-157

and there was downregulation of genes related to the cell cycle and upregulation of genes related to skeletal muscle development observed in the posttreatment tumor cells.

Analysis of the p53 sequence in cancer subject 1* demonstrated a conversion of amino acid 72 proline/proline homozygous alleles in the prebiopsy specimen to arginine/proline heterozygous alleles in the posttreatment normal and tumor tissues (see Supporting Fig. 6). This possibly could be due to APG-157–mediated killing of proline/proline–containing cells in the heterozygous tumor cell population.

Recruitment of Immune Cells to the Tumor Microenvironment After Treatment With APG-157

Hematoxylin and eosin staining of the prebiopsy tumor sample demonstrated the presence of adipocytes, skeletal muscle, nerve cells, and lymphocytes (Fig. 7A). Multiplex immunofluorescence staining showed the presence of scattered CD8-positive cells (Fig. 7B). However, cells that were positive for CD4, PD-1, and PD-L1 were not observed.

After APG-157 treatment, normal tissue (adjacent to the resected tumor) demonstrated the presence of adipocytes, skeletal muscle, nerve cells, and lymphocytes (Fig. 7C). Immunofluorescence staining showed positivity for CD8-positive cells and a few CD4-positive cells (Fig. 7D). There was no staining for PD-1 or PD-L1 expression noted. After treatment with APG-157, hematoxylin and eosin staining of oral tumor tissue demonstrated the presence of salivary gland cells, tumor cells, and fibrous stroma (Fig. 7E). There was a marked increase in the expression of CD8-positive and CD4-positive cells (Fig. 7F). Many of these T cells also were found to be positive for PD-1 expression. Finally, PD-L1 positivity in the tumor cells that were absent in prebiopsy tumor cells also was observed.

Analysis of left and right neck lymph node biopsies after treatment with APG-157 demonstrated the presence of CD8-positive and CD4-positive cells in the paracortex, PD-1–positive staining in the germinal center, and PD-L1–positive staining in the paracortex (see Supporting Figs. 7A-D). These results indicated recruitment of T cells to the tumor microenvironment, possibly attributed to APG-157 treatment.

DISCUSSION

The results of the current study demonstrated that transoral APG-157 treatment leads to systemic absorption of curcumin and its analogs. There was a statistically significant concentration reduction in inflammatory cytokines and *Bacteroides* species noted in the salivary cells. Pretreatment and posttreatment tumor samples from a patients with cancer demonstrated T-cell recruitment to the tumor microenvironment, indicating that APG-157 could be used in an adjuvant treatment setting with checkpoint blockade inhibitors.

Inactivation of p53 (>90%) through mutations in the DNA-binding domain and p16 (>70%) through homozygous deletion and promoter methylation are common events in patients with H&N cancer.[38] Treatments of H&N cancer include surgery and/or chemoradiation with platinum compounds (cisplatin or carboplatin).[6] Cisplatin treatment induces senescence and apoptosis. Although apoptosis results in the suppression of tumor recurrence, senescence could lead to disease recurrence through the expression of senescence-associated proteins, including inflammatory cytokines. Our previous studies demonstrated the elevated concentrations of cytokines in the salivary supernatant fluids of patients with cancer when compared with normal subjects.[33] We also have shown that curcumin inhibits NF-kB activity by retaining the transcription factor in the cytoplasm, which is different from the ubiquitination of NF-kB by cisplatin.[23,38] In the current study, we demonstrated higher concentrations of cytokines in the salivary supernatant fluids of patients with cancer and reduced concentrations after treatment with APG-157, including the proinflammatory cytokines IL-1β and IL-8. Thus, the data from the current study suggest that APG-157 could suppress tumor cell senescence by reducing the concentrations of NF-κB–driven inflammatory cytokines.

The potential benefits of turmeric or curcumin are limited by poor solubility, low absorption from the digestive tract, and rapid systemic elimination.[39] Development of different formulations and changing the route of delivery have resulted in improved bioavailability. A recent study has shown that curcumin delivered in chewing gum form leads to better systemic absorption.[40] Our previous studies have shown that the topical application of curcumin results in a significant reduction in cytokine concentrations as well as the inhibition of xenograft tumor cell growth.[41] In another in vivo study, we demonstrated antitumor effects in preclinical xenograft tumors using liposomal curcumin injected via the tail vein of nude mice.[21] Data from the current study regarding treatment with APG-157 in humans demonstrated that the maximum circulating concentration of curcumin at 3 hours was approximately 10 nM. In the mouse, the maximum circulating concentration was approximately 100 nM.

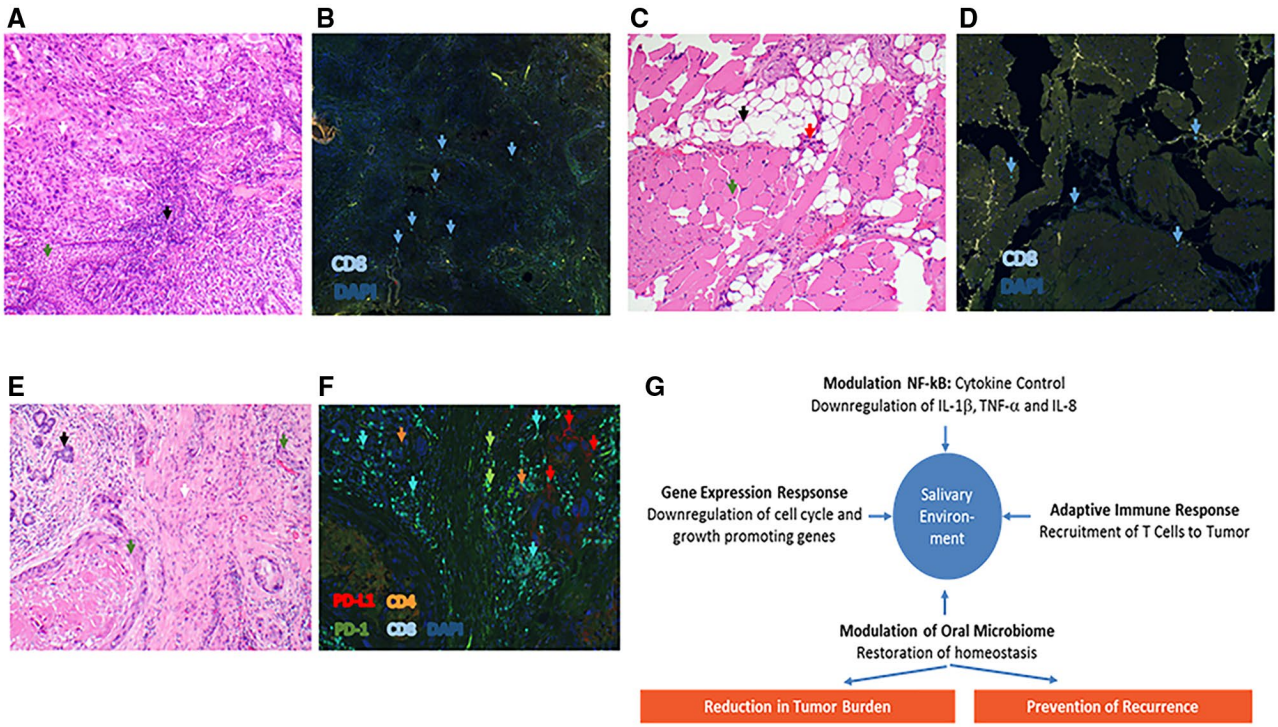

Figure 7. Expression of CD4 and CD8 positive T cells in the post APG-157 treated tumor tissue. (A and C) H & E staining shows the presence of adipocytes (black arrows), skeletal muscle (green arrows), nerve cells (white arrows) and lymphocytes (red arrows) in the pre-biopsy and post treated normal tissues. (B) Scattered CD8 positive T cells (cyan arrows) are seen in the pre-biopsy tumor cells and CD4 positive T cells are absent in these cells. (D) Scattered CD8 positive T cells and absence of CD4, PD-1 and PD-L1 expressing cells are seen in the normal tissue sample. (E) H & E staining of the post treated tumor tissue shows the presence of salivary gland, tumor cells and fibrous stroma represented by black, green and white arrows respectively. (F) PD-L1 (red arrows), PD-1 (green arrows), CD8 (cyan arrows), and CD4 (orange arrows) positive cells points to the expression of PD-L1 in response to T cell infiltration into the tumor microenvironment called, 'adaptive PD-L1 expression' suggesting that immune checkpoint blockade (anti-PD-1 or anti-PD-L1 antibody) could work under these conditions. (G) A model of APG-157 mediated effect points to the inhibitory role of curcumin and its analogs on multiple cell signaling pathways.

Therefore, the circulating concentration of the drug in the human experiment was 10% of the circulating drug concentration in the mice. The 2 experiments should not be compared because of the different routes of drug administration and the different amounts of drug administered. Thus, the unique formulation of APG-157 and its transoral mucosal delivery resulted in the systemic absorption of curcumin and related compounds within 1 hour of treatment (Fig. 1). The observation of systemic and tissue absorption even at the dose of 300 mg (100 mg × 3 for the 3-hour treatment) compared with 8 g per day in food consumption studies[42] indicated that topical application through oral delivery is preferred for curcumin-based human clinical studies.

The results of the current study demonstrated that APG-157 treatment reduces salivary inflammatory cytokines, and this may be directly related to changes in the oral microbiota. Similar to prior reports,[43] the results herein demonstrated that the oral microbiome of patients with cancer is distinct from that of healthy controls (Fig. 3). In the current study, we found that 33 genera are differentially abundant in patients with cancer compared with healthy controls. *Fusicatenibacter* was the most abundant genus that was underrepresented in patients with cancer, whereas the most abundant genera that were overrepresented in patients with cancer included *Dorea*, *Ruminococcus*, *Dialister*, *Parabacteroides*, *Ruminoclostridium*, and *Alistipes*. The overabundance of genera such as *Dorea* and *Alistipes* is consistent with prior studies that have compared the oral microbiome of patients with H&N cancer with that of control subjects.[32] Taxonomical studies have suggested *Alistipes* species as a tumor-promoting bacteria in colon cancer through increased IL-6 signaling.[44] The findings of the current study support the possibility that the oral microbiome plays a role in the pathogenesis of H&N cancer. Therefore, it may be possible to influence disease outcome by modulating the oral microbiome.

The results of the current study demonstrate that the administration of APG-157 distinctly alters the oral microbiome by significantly decreasing *Bacteroides* (Fig. 4). Previously, *Bacteroides* has been implicated in colon cancer by both human association studies and mouse models in which *Bacteroides* colonization increased colon cancer susceptibility.[45] There may be a direct relationship between these changes and reduced inflammatory cytokine levels in saliva that may benefit patients with cancer when they are treated for a longer duration. Therefore, the findings of the current study offer promising preliminary data to support the hypothesis that APG-157 has an anticancer effect through a microbiome-mediated pathway.

Multiplex immunofluorescence analysis demonstrated immune cell infiltration (increased expression of CD4-positive and CD8-positive cells) in tumor cells after treatment in comparison with the prebiopsy sample (Fig. 6). There also was increased expression of PD-1 and PD-L1 in the tumor boundary of tumors after treatment with APG-157. Thus, there was immune cell infiltration in the tumor microenvironment within 48 hours of receipt of APG-157. Increased T cells also were observed in posttreatment lymph nodes. However, normal tissue did not demonstrate any immune cell infiltration. Therefore, APG-157 has potential use for combination therapy with immune checkpoint blockade, given the increased immune cell infiltration and increased PD-L1 expression that likely represents an adaptive immune resistance.[46,47]

Expression levels of various chemokines are known to be associated with immune cell infiltration in the tumor microenvironment. In the RNA-Seq analysis of CC and CXC chemokine expression, increased expression of CCL2, CCL11, CCL19, CCL28 and CXCL1, CXCL5, and CXCL8 with downregulation of CXCL2, CXCL12, and CXCL13 was observed in the posttreatment tumor sample (see Supporting Figs. 7E and F). CCL2 expression was correlated with CD3-positive, CD8-positive T-cell infiltration in several studies.[48] CCL2, CXCL5, CXCL8, and CXCL12 are suggested to play a role in monocyte recruitment in the tumor microenvironment, and CCL28 is involved in regulatory T cell recruitment that may be associated with the promotion of immune evasion. Thus, it is speculated that chemokine expression changes after treatment with APG-157 may have led to the recruitment of CD4 and CD8 T cells in the tumor microenvironment (Fig. 7G). This suggests that APG-157 therapy has the potential to attract immune cells to the tumor microenvironment and provides a strong rationale for the use of immune checkpoint blockade to block T cell and tumor cell interaction (PD-1/PD-L1 axis), which to the best of our knowledge is the most well-characterized immune evasive immune checkpoint. Furthermore, in vivo mouse studies will be necessary to understand the mechanistic insight of T-cell recruitment to the tumor microenvironment. The results indicate that a long-term evaluation of immune checkpoint blockade with and without APG-157 could provide a clear understanding of the usefulness of APG-157 as either an adjuvant or neoadjuvant therapeutic agent for patients with advanced or recurrent H&N cancer.

FUNDING SUPPORT

Funding was received from Aveta Biomics Inc and the University of California at Los Angeles Academic Senate as well as the Veterans Administration Greater Los Angeles Healthcare System West Los Angeles surgical education program (to Eri S. Srivatsan and Marilene B. Wang).

CONFLICT OF INTEREST DISCLOSURES

Sharmila Mudgal was Chief Medical Officer of Aveta Biomics Inc, which partially funded the current study, and has a patent pending for Polypharmaceutical Drug Compositions and Related Methods. Parag Mehta and Luis Avila are employees of Aveta Biomics Inc, which provided partial funding for the current study, and have a patent pending for Polypharmaceutical Drug Compositions and Related Methods. Sharmila Mudgal, Parag Mehta, and Luis Avila had no role in the recruitment of the subjects and collection and analysis of the samples. All authors were blinded to the study and its results until the study was completed. The other authors made no disclosures.

AUTHOR CONTRIBUTIONS

Saroj K. Basak: Conceptualization, data curation, investigation, methodology, project administration, writing–original draft, and writing–review and editing. **Alakesh Bera:** Data curation, investigation, methodology, validation, visualization, and writing–review and editing. **Alexander J. Yoon:** Data curation, investigation, methodology, validation, visualization, and writing–review and editing. **Marco Morselli:** Data curation, investigation, methodology, supervision, validation, writing–original draft, and writing–review and editing. **Chan Jeong:** Data curation, investigation, methodology, and writing–original draft. **Anela Tosevska:** Data curation, investigation, methodology, validation, visualization, writing–original draft, and writing–review and editing. **Tien S. Dong:** Investigation, methodology, validation, writing–original draft, and writing–review and editing. **Michael Eklund:** Data curation, formal analysis, methodology, validation, and writing–review and editing. **Eric Russ:** Data curation, investigation, methodology, validation, visualization, and writing–review and editing. **Hassan Nasser:** Data curation, investigation, and methodology. **Venu Lagishetty:** Investigation, methodology, validation, and visualization. **Rong Guo:** Formal analysis, software, validation, visualization, and writing–original draft. **Dipti Sajed:** Investigation, methodology, validation, and writing–review and editing. **Sharmila Mudgal:** Conceptualization, funding acquisition, project administration, resources, and writing–review and editing. **Parag Mehta:** Conceptualization, funding acquisition, project administration, resources, and writing–review and editing. **Luis Avila:** Conceptualization, funding acquisition, project administration, resources, and writing–review and editing. **Meera Srivastava:** Data curation, formal analysis, investigation, methodology, supervision, validation, visualization, writing–original draft, and writing–review and editing. **Kym Faull:** Investigation, methodology, supervision, validation, writing–original draft, and writing–review and editing. **Jonathan Jacobs:** Investigation, methodology, supervision, and writing–review and editing. **Matteo Pellegrini:** Methodology, supervision, validation, visualization, writing–original draft, and writing–review and editing. **Daniel Sanghoon Shin:** Conceptualization, investigation, methodology, validation, visualization,

writing–original draft, and writing–review and editing. **Eri S. Srivatsan:** Conceptualization, investigation, methodology, project administration, supervision, validation, visualization, writing–original draft, and writing–review and editing. **Marilene B. Wang:** Conceptualization, project administration, supervision, validation, visualization, writing–original draft, and writing–review and editing.

REFERENCES

1. Gandini S, Botteri E, Iodice S, et al. Tobacco smoking and cancer: a meta-analysis. *Int J Cancer*. 2008;122:155-164.
2. Bray F, Ferlay J, Soerjomataram I, Siegel RL, Torre LA, Jemal A. Global cancer statistics 2018: GLOBOCAN estimates of incidence and mortality worldwide for 36 cancers in 185 countries. *CA Cancer J Clin*. 2018;68:394-424. doi:10.3322/caac.21492
3. Cancer.Net. Head and Neck Cancer: Statistics. Accessed April 1, 2019. https://www.cancer.net/cancer-types/head-and-neck-cancer/statistics
4. Siegel RL, Miller KD, Jemal A. Cancer statistics, 2019. *CA Cancer J Clin*. 2019;69:7-34. doi:10.3322/caac.21551
5. Siegel RL, Miller KD, Jemal A. Cancer statistics, 2017. *CA Cancer J Clin*. 2017;67:7-30.
6. Go RS, Adjei AA. Review of the comparative pharmacology and clinical activity of cisplatin and carboplatin. *J Clin Oncol*. 1999;17:409-422.
7. Fury MG, Sherman EJ, Rao SS, et al. Phase I study of weekly nab-paclitaxel + weekly cetuximab + intensity-modulated radiation therapy (IMRT) in patients with stage III-IVB head and neck squamous cell carcinoma (HNSCC). *Ann Oncol*. 2014;25:689-694.
8. Guardiola E, Peyrade F, Chaigneau L, et al. Results of a randomised phase II study comparing docetaxel with methotrexate in patients with recurrent head and neck cancer. *Eur J Cancer*. 2004;40:2071-2076.
9. Jacobs C, Lyman G, Velez-Garcia E, et al. A phase III randomized study comparing cisplatin and fluorouracil as single agents and in combination for advanced squamous cell carcinoma of the head and neck. *J Clin Oncol*. 1992;10:257-263.
10. Vermorken JB, Trigo J, Hitt R, et al. Open-label, uncontrolled, multicenter phase II study to evaluate the efficacy and toxicity of cetuximab as a single agent in patients with recurrent and/or metastatic squamous cell carcinoma of the head and neck who failed to respond to platinum-based therapy. *J Clin Oncol*. 2007;25:2171-2177.
11. Ferris RL, Blumenschein G Jr, Fayette J, et al. Nivolumab vs investigator's choice in recurrent or metastatic squamous cell carcinoma of the head and neck: 2-year long-term survival update of CheckMate 141 with analyses by tumor PD-L1 expression. *Oral Oncol*. 2018;81:45-51. doi:10.1016/j.oraloncology.2018.04.008
12. Cohen EEW, Soulieres D, Le Tourneau C, et al; KEYNOTE-040 investigators. Pembrolizumab versus methotrexate, docetaxel, or cetuximab for recurrent or metastatic head-and-neck squamous cell carcinoma (KEYNOTE-040): a randomised, open-label, phase 3 study. *Lancet*. 2019;393:156-167. doi:10.1016/S0140-6736(18)31999-8
13. Zhang X, Yang H, Lee JJ, et al. MicroRNA-related genetic variations as predictors for risk of second primary tumor and/or recurrence in patients with early-stage head and neck cancer. *Carcinogenesis*. 2010;31:2118-2123. doi:10.1093/carcin/bgq177
14. Forster MD, Devlin MJ. Immune checkpoint inhibition in head and neck cancer. *Front Oncol*. 2018;8:310. doi:10.3389/fonc.2018.00310
15. Price KA, Cohen EE. Current treatment options for metastatic head and neck cancer. *Curr Treat Options Oncol*. 2012;13:35-46. doi:10.1007/s11864-011-0176-y
16. Nelson KM, Dahlin JL, Bisson J, Graham J, Pauli GF, Walters MA. The essential medicinal chemistry of curcumin. *J Med Chem*. 2017;60:1620-1637. doi:10.1021/acs.jmedchem.6b00975
17. Wong KE, Ngai SC, Chan KG, Lee LH, Goh BH, Chuah LH. Curcumin nanoformulations for colorectal cancer: a review. *Front Pharmacol*. 2019;10:152. doi:10.3389/fphar.2019.00152
18. Wilken R, Veena MS, Wang MB, Srivatsan ES. Curcumin: a review of anti-cancer properties and therapeutic activity in head and neck squamous cell carcinoma. *Mol Cancer*. 2011;10:12. doi:10.1186/1476-4598-10-12
19. Allegra A, Innao V, Russo S, Gerace D, Alonci A, Musolino C. Anticancer activity of curcumin and its analogues: preclinical and clinical studies. *Cancer Invest*. 2017;35:1-22. doi:10.1080/07357907.2016.1247166
20. Mimeault M, Batra SK. Potential applications of curcumin and its novel synthetic analogs and nanotechnology-based formulations in cancer prevention and therapy. *Chin Med*. 2011;6:31. doi:10.1186/1749-8546-6-31
21. Wang D, Veena MS, Stevenson K, et al. Liposome-encapsulated curcumin suppresses growth of head and neck squamous cell carcinoma in vitro and in xenografts through the inhibition of nuclear factor kappaB by an AKT-independent pathway. *Clin Cancer Res*. 2008;14:6228-6236. doi:10.1158/1078-0432.CCR-07-5177
22. Basak SK, Zinabadi A, Wu AW, et al. Liposome encapsulated curcumin-in-difluorinated (CDF) inhibits the growth of cisplatin resistant head and neck cancer stem cells. *Oncotarget*. 2015;6:18504-18517.
23. Duarte VM, Han E, Veena MS, et al. Curcumin enhances the effect of cisplatin in suppression of head and neck squamous cell carcinoma via inhibition of IKKβ protein of the NFκB pathway. *Mol Cancer Ther*. 2010;9:2665-2675. doi:10.1158/1535-7163.MCT-10-0064
24. Adiwidjaja J, McLachlan AJ, Boddy AV. Curcumin as a clinically-promising anti-cancer agent: pharmacokinetics and drug interactions. *Expert Opin Drug Metab Toxicol*. 2017;13:953-972. doi:10.1080/17425255.2017.1360279
25. Morin D, Barthelemy S, Zini R, Labidalle S, Tillement JP. Curcumin induces the mitochondrial permeability transition pore mediated by membrane protein thiol oxidation. *FEBS Lett*. 2001;495:131-136.
26. Piwocka K, Zablocki K, Wieckowski MR, et al. A novel apoptosis-like pathway, independent of mitochondria and caspases, induced by curcumin in human lymphoblastoid T (Jurkat) cells. *Exp Cell Res*. 1999;249:299-307.
27. Meurman JH. Oral microbiota and cancer. *J Oral Microbiol*. 2010;2. doi:10.3402/jom.v2i0.5195
28. Allavena P, Garlanda C, Borrello MG, Sica A, Mantovani A. Pathways connecting inflammation and cancer. *Curr Opin Genet Dev*. 2008;18:3-10. doi:10.1016/j.gde.2008.01.003
29. Lim Y, Fukuma N, Totsika M, Kenny L, Morrison M, Punyadeera C. The performance of an oral microbiome biomarker panel in predicting oral cavity and oropharyngeal cancers. *Front Cell Infect Microbiol*. 2018;8:267. doi:10.3389/fcimb.2018.00267
30. Yang SF, Huang HD, Fan WL, et al. Compositional and functional variations of oral microbiota associated with the mutational changes in oral cancer. *Oral Oncol*. 2018;77:1-8. doi:10.1016/j.oraloncology.2017.12.005
31. Yang CY, Yeh YM, Yu HY, et al. Oral microbiota community dynamics associated with oral squamous cell carcinoma staging. *Front Microbiol*. 2018;9:862. doi:10.3389/fmicb.2018.00862
32. Lee WH, Chen HM, Yang SF, et al. Bacterial alterations in salivary microbiota and their association in oral cancer. *Sci Rep*. 2017;7:16540. doi:10.1038/s41598-017-16418-x
33. Kim SG, Veena MS, Basak SK, et al. Curcumin treatment suppresses IKKβ kinase activity of salivary cells of patients with head and neck cancer: a pilot study. *Clin Cancer Res*. 2011;17:5953-5961. doi:10.1158/1078-0432.CCR-11-1272
34. Jacobs JP, Lin L, Goudarzi M, et al. Microbial, metabolomic, and immunologic dynamics in a relapsing genetic mouse model of colitis induced by T-synthase deficiency. *Gut Microbes*. 2017;8:1-16. doi:10.1080/19490976.2016.1257469
35. Love MI, Huber W, Anders S. Moderated estimation of fold change and dispersion for RNA-seq data with DESeq2. *Genome Biol*. 2014;15:550.
36. Storey JD, Tibshirani R. Statistical significance for genomewide studies. *Proc Natl Acad Sci U S A*. 2003;100:9440-9445.
37. Carithers LJ, Ardlie K, Barcus M, et al; GTEx Consortium. A novel approach to high-quality postmortem tissue procurement: the GTEx project. *Biopreserv Biobank*. 2015;13:311-319.
38. Veena MS, Wilken R, Zheng JY, et al. p16 protein and gigaxonin are associated with the ubiquitination of NFκB in cisplatin-induced senescence of cancer cells. *J Biol Chem*. 2014;289:34921-34937. doi:10.1074/jbc.M114.568543
39. Toden S, Goel A. The holy grail of curcumin and its efficacy in various diseases: is bioavailability truly a big concern? *J Restor Med*. 2017;6:27-36. doi:10.14200/jrm.2017.6.0101
40. Boven L, Holmes SP, Latimer B, et al. Curcumin gum formulation for prevention of oral cavity head and neck squamous cell carcinoma. *Laryngoscope*. 2019;129:1597-1603. doi:10.1002/lary.27542

41. LoTempio MM, Veena MS, Steele HL, et al. Curcumin suppresses growth of head and neck squamous cell carcinoma. *Clin Cancer Res*. 2005;11(19 pt 1):6994-7002.
42. Dhillon N, Aggarwal BB, Newman RA, et al. Phase II trial of curcumin in patients with advanced pancreatic cancer. *Clin Cancer Res*. 2008;14:4491-4499. doi:10.1158/1078-0432.CCR-08-0024
43. Hayes RB, Ahn J, Fan X, et al. Association of oral microbiome with risk for incident head and neck squamous cell cancer. *JAMA Oncol*. 2018;4:358-365. doi:10.1001/jamaoncol.2017.4777
44. Moschen AR, Gerner RR, Wang J, et al. Lipocalin 2 protects from inflammation and tumorigenesis associated with gut microbiota alterations. *Cell Host Microbe*. 2016;19:455-469. doi:10.1016/j.chom.2016.03.007
45. Purcell RV, Pearson J, Aitchison A, Dixon L, Frizelle FA, Keenan JI. Colonization with enterotoxigenic Bacteroides fragilis is associated with early-stage colorectal neoplasia. *PLoS One*. 2017;12:e0171602. doi:10.1371/journal.pone.0171602
46. Ribas A. Releasing the brakes on cancer immunotherapy. *N Engl J Med*. 2015;373:1490-1492. doi:10.1056/NEnglJMed.p1510079
47. Smyth MJ, Ngiow SF, Ribas A, Teng MW. Combination cancer immunotherapies tailored to the tumour microenvironment. *Nat Rev Clin Oncol*. 2016;13:143-158. doi:10.1038/nrclinonc.2015.209
48. Shields BD, Mahmoud F, Taylor EM, et al. Indicators of responsiveness to immune checkpoint inhibitors. *Sci Rep*. 2017;7:807. doi:10.1038/s41598-017-01000-2